NANO LETTERS

xxxx
Vol. 0, No. 0
A−E

Directional Control in Thermally Driven Single-Molecule Nanocars

Yasuhiro Shirai,[†] Andrew J. Osgood,[‡] Yuming Zhao,[†] Kevin F. Kelly,*[,‡] and James M. Tour*[,†]

Departments of Chemistry, Mechanical Engineering, and Materials Science, Center for Nanoscale Science and Technology, Department of Electrical and Computer Engineering, and Rice Quantum Institute, Rice University, Houston, Texas 77005

Received September 26, 2005

ABSTRACT

With the hope of directing future bottom-up fabrication through bulk external stimuli (such as electric fields) on nanometer-sized transporters, we sought to study controlled molecular motion on surfaces through the rational design of surface-capable molecular structures called nanocars. Here we show that the observed movement of the nanocars is a new type of fullerene-based wheel-like rolling motion, not stick–slip or sliding translation, due to evidence including directional preference in both direct and indirect manipulation and studies of related molecular structures.

The thrust to design single-molecule-sized nanoscale machines with controlled mechanical motion has yielded a variety of molecular machinery resembling macroscopic motors, switches, shuttles, turnstiles, gears, bearings, gyroscopes, and elevators.[1−3] In most cases, the nanomachines have been operated and observed spectroscopically as ensembles of molecules in the solution phase. In some instances, however, molecules such as benzene,[4] porphyrins,[5] fullerene-C_{60},[6] a cyclodextrin necklace,[7] molecular landers,[8] and altitudinal molecular rotors[9] have been treated as individual molecules on solid surfaces using a scanning tunneling microscope (STM). Most observed tangential motion of these latter systems has been attributed to a stick−slip or sliding movement.[10] An exception to this are fullerene structures (C_{60} and carbon nanotubes) that are theorized[11−13] and have been shown[14−19] to exhibit rolling translation and rotation on various surfaces because of their highly symmetric, closed graphene structures. With the hope of directing future bottom-up fabrication through bulk external stimuli (such as electric fields) on nanometer-sized transporters, we sought to study controlled molecular motion on surfaces through the rational design of surface-capable molecular structures called nanocars. Here we show that the observed movement of the nanocars is a new type of fullerene-based wheel-like rolling motion, not stick−slip or sliding translation, due to evidence including directional preference in both direct and indirect manipulation and studies of related molecular structures.

* Corresponding authors. E-mail: tour@rice.edu; kkelly@rice.edu.
[†] Departments of Chemistry, Mechanical Engineering, and Materials Science and Center for Nanoscale Science and Technology.
[‡] Department of Electrical and Computer Engineering and Rice Quantum Institute.

The design and synthesis of the nanocar molecule was directed to enable controllable surface transport by means of the rotation of wheel-like fullerenes (Figure 1).[20] Although mass orchestrated motion is an eventual goal, it was necessary to examine individual molecules to determine the functional mode of surface transport. At approximately 3 × 4 nm each, these molecules are ideal candidates for individual study by STM. Several different versions and derivatives have been synthesized and studied, but the focus here is on nanocar **1**, with similar trimer molecules **2** and **3** offering supporting evidence.

The sample preparation and data collection for the STM study were performed as follows: The nanocars (**1**) were suspended in toluene (5 μM) and initially spun-cast on Au(111) on mica and imaged in an ambient, home-built STM. Following initial investigations in air, the toluene solution of **1** was dosed in high vacuum using a fast-actuating, small orifice solenoid valve[22,23] onto argon-sputtered and annealed Au(111) on mica substrates and imaged using an RHK variable temperature UHV-STM. The dosing technique was chosen over sublimation in vacuum because it appeared in thermal decomposition studies using a thermogravimetric analyzer on related oligo(phenylene ethynylene) (OPE) alkynyl-fullerenes that the fullerene-based wheels began to cleave from the alkynyl-axles at ca. 300 °C with rapid decomposition occurring by 350 °C. A piece of silicon, placed directly underneath the gold substrate, was resistively heated to perform variable temperature studies in the STM. The sample temperature was measured by a K-type thermocouple wire placed directly on the gold surface.

The nanocars (**1**) were distributed randomly across the Au(111) terraces and monatomic step edges (Figure 2a).

10.1021/nl051915k CCC: $30.25 © xxxx American Chemical Society
Published on Web 00/00/0000

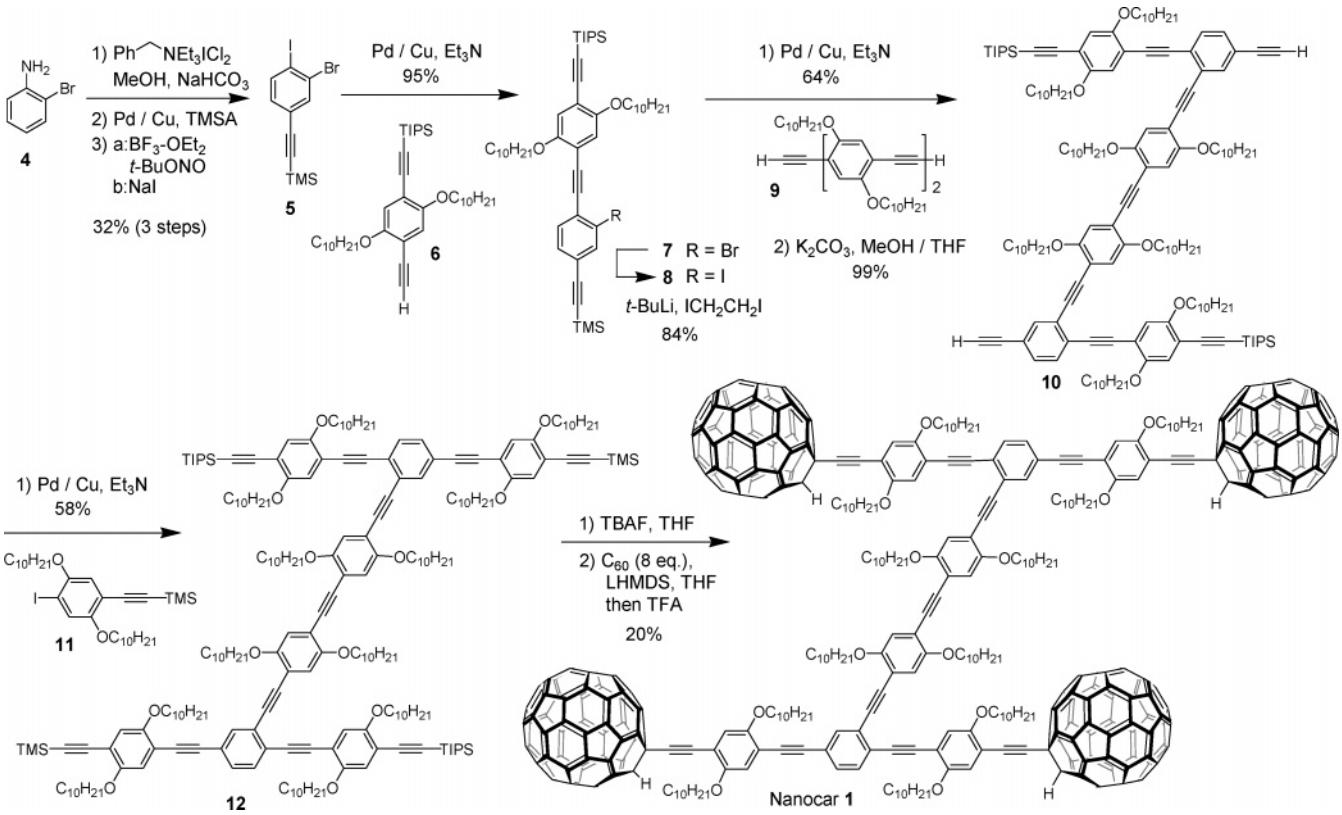

Figure 1. Synthesis and structure of nanocar **1**. The synthesis of nanocar **1** involves extensive Pd-catalyzed coupling reactions, and four fullerene "wheels" were attached in one reaction step.[21] Structure was definitively characterized spectroscopically.[20] Through the synthesis and study of several related structures including trimers **2** and **3**, it was clear that the alkyl units were critical for the requisite solubility of these molecules. Fullerene wheels and chassis parts can rotate because of the alkyne connections, giving the nanocar the ability to roll on the surface and flexibility orthogonal to the surface plane.

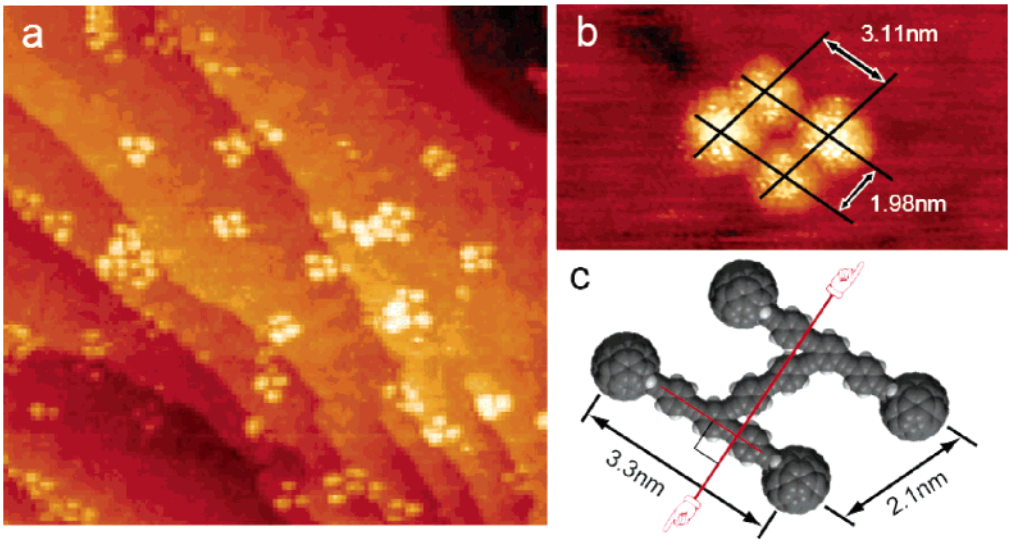

Figure 2. Nanocar **1** on Au(111) surface. (a) STM image (bias voltage [V_b] = 0.4 V, tunneling current [I_t] = 10 pA; image size is 73 × 70 nm^2) of the nanocars (**1**) deposited on Au(111) by dosing valve. Bright features are fullerene wheels; intramolecular OPE and alkyl groups are not visible. (b) High-resolution STM image (V_b = 0.4 V, I_t = 60 pA). The orientation of the molecules can be determined by the fullerene peak-to-peak distances, with (c) modeled distances at 3.3 nm across the width and 2.1 nm across the length, or the axle and chassis directions, respectively, as shown in this alkyl-free space-filling model. The red fingers indicate the expected direction of rolling perpendicular to the axles.

Initial imaging demonstrated that the nanocars (**1**) were stable and stationary on the gold surface at room temperature for a wide range of tunneling parameters. We attribute their stability to a relatively strong adhesion force between the fullerene wheels and the underlying gold. This type of bonding for fullerenes on metals has been observed previously and investigated by a wide variety of surface science techniques.[24−26] Because of their rectangular (not square)

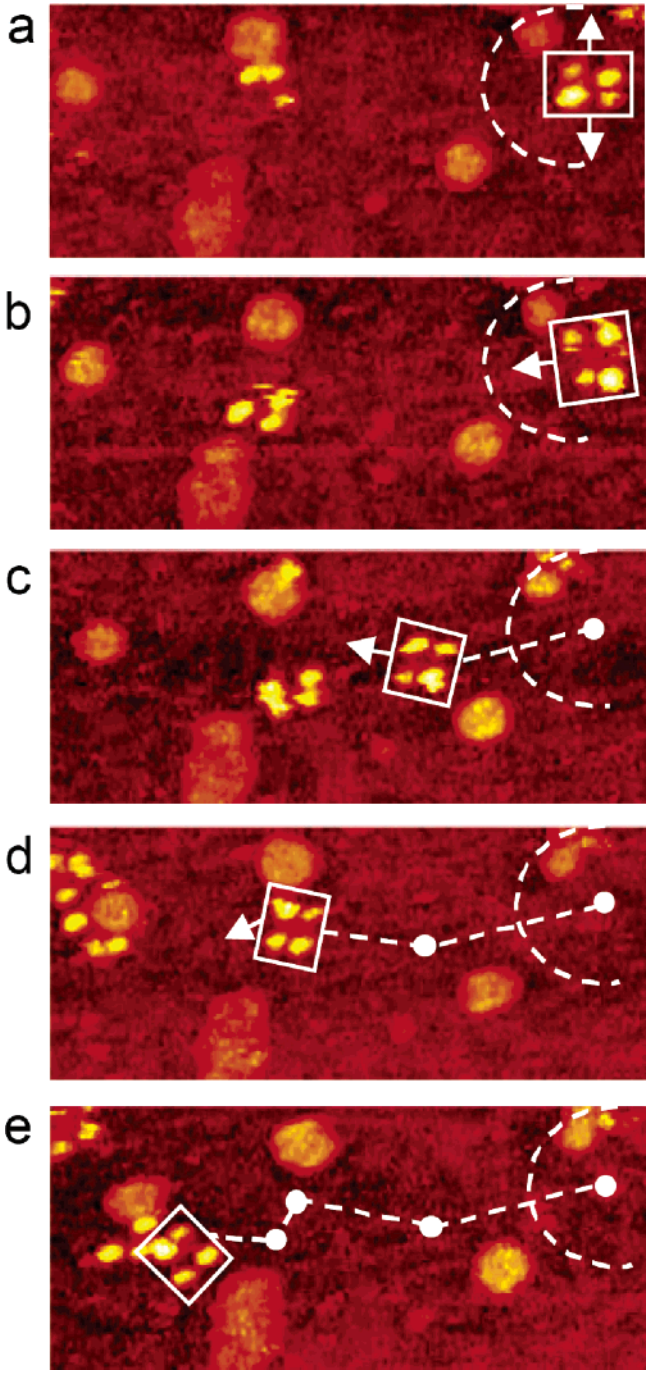

Figure 3. Nanocar **1** rolling on Au surface. (a−e). A small section of a sequence of images taken during annealing at ∼200 °C ($V_b = -0.95$ V, $I_t = 200$ pA; image size is 51 × 23 nm^2). The orientation of **1** is determined easily by the fullerene wheel separation, with motion occurring perpendicular to the axles. The acquisition time for each image is approximately 1 min, with a−e selected from a series spanning 10 min, which shows ∼80° pivot (a) followed by translation interrupted by small-angle pivot perturbations (b−e). See http://tourserver.rice.edu/movies/ for the complete video file and interstitial images.

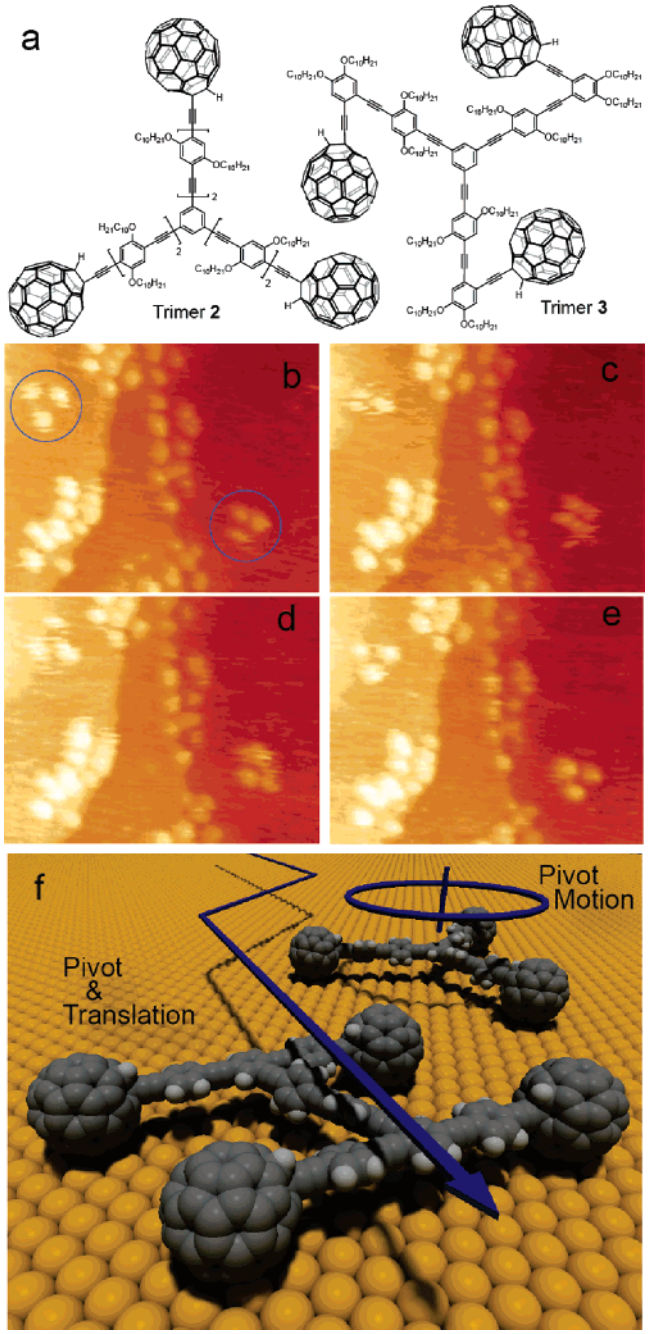

Figure 4. Structure and pivot motion of the trimers. (a) Structure of trimers **2** and **3**. A sequence of STM images (b−e) acquired approximately 1 min apart during annealing at ∼225 °C show the pivoting motion of **2** (both circled molecules) and lack of translation in b−e of any molecules. These images were taken from a much longer sequence at the same temperature, a part of which can be found on http://tourserver.rice.edu/movies/ ($V_b = -0.7$ V, $I_t = 200$ pA; image size is 34 × 27 nm^2). Monatomic step edges in these images are lined with clustered molecules. (f) A summary of the two methods of motion for the different structures showing that nanocar **1** consecutively pivots and then translates perpendicular to its axles, whereas trimer **2** pivots but does not translate on the surface. For clarity, both structures are drawn devoid of the alkoxy units.

constitution, determination of the chassis and axle orientation of the four-lobed molecules was possible through peak-to-peak length versus width measurements. The fullerene wheels are brightly imaged and thereby provide a definitive indication of the molecule and its orientation (Figure 2b and c). The internal OPE and alkyl structure is not visible under the imaging conditions tested, a range of 3−300 pA and 2 mV to 2.0 V at either bias polarity. The peculiarity of transparency of the OPE axles and chassis for the nanocars (**1**), and related two-wheeled (see the Supporting Information)

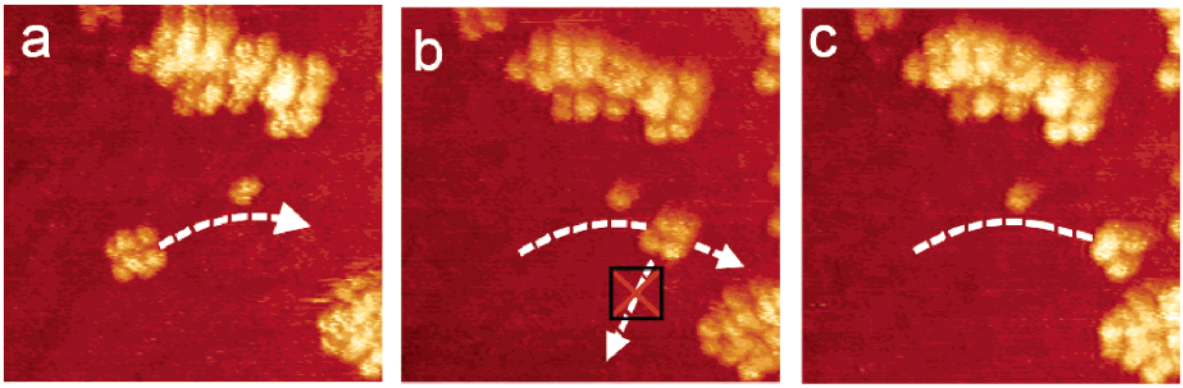

Figure 5. Direct STM manipulation of nanocar **1**. A single nanocar **1** is pulled with the tip perpendicular to its axles (30 pA, 0.1 V imaging conditions; 3.5 nA, 0.1 V manipulation conditions). The tip was lowered in front of the molecule in the direction of motion and pulled from image a to b. After b, the same technique failed to move nanocar **1** when the tip was lowered to the side and dragged away at 90° to its previous motion. (c) Nanocar **1** was then moved with the same technique further along its initial path before it appeared to pivot 90° to its original orientation after approaching the other nanocars on the lower right of the image.

and three-wheeled structures (**2** and **3**), is a consistent trend, and such phenomena in STM imaging have been discussed previously.[27,28]

After imaging at room-temperature, the substrate temperature was slowly increased while still maintaining the tunnel junction. The nanocars (**1**) remained effectively stationary on the surface up to approximately 170 °C. As the temperature increased above this point, the molecules began to move in two dimensions through a combination of both translation and pivoting, not in the 1D manner initially expected. For example, at approximately 200 °C, the motion of the nanocars (**1**) is, on average, slow enough to be followed through a series of 1-min images. Pivoting motion can be seen in a sequence of images (Figure 3a−e). The translational motion that occurred between pivoting was perpendicular to the axles, illustrating a directional preference relative to the molecular orientation. A supplemental movie for this series of images can be found at our website. (Two STM movies are available at http://tourserver.rice.edu/movies/. Nanocar zoom movie: nanocar **1** on Au(111) annealed at 200 °C moving perpendicular to axles; trimers movie: 50:50 mixed trimers **2** and **3** on Au(111) annealed at 225 °C, zoomed.) The observed 2D motion of the molecules, instead of the expected 1D motion, can be explained by the ability of the fullerenes to rotate independently of one another, giving rise to a pivoting motion of the molecule on the small atomic corrugation of a Au(111) substrate. Even though the motion is 2D, imaging at these elevated temperatures shows that the translational movement of the nanocars (**1**) occurs in the direction perpendicular to their axles. Above approximately 225 °C, the rapid and erratic motion of the molecules could not be tracked because of the relatively slow acquisition time necessary (approximately 1 min for a 90 × 90 nm^2 scan) compared to the rate of surface diffusion of the molecules.

To further explore the hypothesis of fullerene-facilitated rolling of the nanocars, two three-wheeled structures (**2** and **3**) (Figure 4a) have been designed and synthesized so that their axles inhibit concerted translational rolling, as in **2**, or any coordinated rolling as in **3**. When **2** and **3** were heated slowly to 225 °C (a higher temperature than needed to induce significant translational motion in the nanocars) only occasional surface diffusion was observed and only a few nanometers distance over 20−30 min of monitoring. The majority of motion of these molecules was of **2** pivoting in place around a central pivot point (Figure 4b−e). No significant translation or pivoting motion of trimer **3** was observed. This behavior was continued up to 300 °C (nearing the onset temperature for decomposition as studied by thermogravimetric analysis) a temperature at which the four-wheeled nanocars (**1**) were moving too quickly to even be imaged by the STM used. One would expect the energy barrier for sliding or stick−slip motion for **2** and **3** to be comparable or even less than that for **1** given there is one less fullerene in **2** and **3** and thus a weaker overall interaction between the molecule and the gold surface. However, because **2** and **3** exhibited little to none of the thermally induced translation over the temperature range investigated, this further suggests that the motion of nanocars (**1**) is due to rolling of the fullerene wheels. The differing motions between **1** and **2** are illustrated in Figure 4f.

Additionally, direct manipulation of **1** by the STM tip was performed in order to further explore the hypothesis that the motion of these molecules is facilitated by rotation of the fullerenes about the alkynyl axles. An example of direct manipulation results and parameters are shown in Figure 5a−c. An immediately noticeable characteristic of the manipulation of these molecules was the fact that for most successful attempts, the tip was lowered in front of the molecule in the direction of motion, meaning that the molecule was pulled by the tip. Pushing attempts never caused nanocar **1** movement in the direction of the tip motion; nanocars (**1**) were always pushed to the side and/or made to pivot. This is atypical of STM molecular manipulation where pushing is almost universally the case with large organic molecules.[29,30] Nanocar **1** was pulled in a shallow arc in a direction perpendicular to its axles (Figure 5a and b), then an attempt was made to pull the nanocar **1** in a direction parallel to its axles, or at 90° to its former path (Figure 5b). This unsuccessful attempt was then followed by a short pulling manipulation again perpendicular to the axles, after

which nanocar **1** rotated 90°, perhaps because of its final proximity to the group of molecules in the lower right-hand corner (Figure 5c). This sequence of manipulation data illustrates a strong directional preference favoring motion perpendicular to the axles, as expected for fullerene-facilitated rolling.

The studies here underscore the ability to control the directionality of motion in molecular-sized nanostructures through precise molecular synthesis. The use of spherical wheels based on fullerene-C_{60} and freely rotating axles based on alkynes permits directed nanoscale rolling of a molecular structure. Further studies are concentrating on electric field-induced motion of nanocars and nanotrains and the use of nanotrucks for assisted small molecule transport across surfaces.

Acknowledgment. This work was funded by the Welch Foundation, Zyvex Corporation, and the NSF Penn State MRSEC. We acknowledge Yu-Hung Chiu, Yuxing Yao, Hanbiao Yang, and Lionel Saudan for their seminal work in the synthesis of previous versions of the nanocar, Tomi Hashizume and Yasuhiko Terada for their expertise in vacuum deposition with the solenoid pulse valve, and Paul Weiss for his insight concerning the STM investigation of these molecules.

Supporting Information Available: STM images of two-wheeled molecules. This material is available free of charge via the Internet at http://pubs.acs.org.

References

(1) Balzani, V.; Credi, A.; Venturi, M. *Molecular Devices and Machines: A Journey into the Nano World*; WILEY-VCH, Weinheim, Germany, 2004.
(2) Kottas, G. S.; Clarke, L. I.; Horinek, D.; Michl, J. *Chem. Rev.* **2005**, *105*, 1281−1376.
(3) (a) Badjić, J. D.; Balzani, V.; Credi, A.; Silvi, S.; Stoddart, J. F. *Science* **2004**, *303*, 1845−1849. (b) Garcia-Garibay, M. A. *Proc. Natl. Acad. Sci. U.S.A.* **2005**, *102*, 10771−10776.
(4) Han, P.; Mantooth, B. A.; Sykes, E. C. H.; Donhauser, Z. J.; Weiss, P. S. *J. Am. Chem. Soc.* **2004** *126*, 10787−10793.
(5) Moresco, F.; Meyer, G.; Rieder, K.-H.; Tang, H.; Gourdon, A.; Joachim, C. *Appl. Phys. Lett.* **2001**, *78*, 306−308.
(6) Guo, S.; Fogarty, D. P.; Nagel, P. M.; Kandel, S. A. *J. Phys. Chem. B* **2004**, *108*, 14074−14081.
(7) Shigekawa, H.; Miyake, K.; Sumaoka, J.; Harada, A.; Komiyama, M. *J. Am. Chem. Soc.* **2000**, *122*, 5411−5412.
(8) Rosei, F.; Schunack, M.; Jiang, P.; Gourdon, A.; Legsgaard, E.; Stensgaard, I.; Joachim, C.; Besenbacher, F. *Science* **2002**, *296*, 328−331.
(9) Zheng, X.; Mulcahy, M. E.; Horinek, D.; Galeotti, F.; Magnera, T. F.; Michl, J. *J. Am. Chem. Soc.* **2004**, *126*, 4540−4542.
(10) Rosei, F.; Schunack, M.; Naitoh, Y.; Jiang, P.; Gourdon, A.; Laegsgaard, E.; Stensgaard, I.; Joachim, C.; Besenbacher, F. *Prog. Surf. Sci.* **2003**, *71*, 95−146.
(11) Hobbs, C.; Kantorovich, L. *Nanotechnology* **2004**, *15*, S1−S4.
(12) Buldum, A.; Lu, J. P. *Phys. Rev. Lett.* **1999**, *83*, 5050−5053.
(13) Ni, B.; Sinnott, S. B. *Surf. Sci.* **2001**, *487*, 87−96.
(14) Keeling, D. L.; Humphry, M. J.; Fawcett, R. H. J.; Beton, P. H.; Hobbs, C.; Kantorovich, L. *Phys. Rev. Lett.* **2005**, *94*, 146104/1−146104/4.
(15) Miura, K.; Kamiya, S.; Sasaki, N. *Phys. Rev. Lett.* **2003**, *90*, 055509.
(16) Miura, K.; Takagi, T.; Kamiya, S.; Sahashi, T.; Yamauchi, M. *Nano Lett.* **2001**, *1*, 161−163.
(17) Falvo, M. R.; Taylor, R. M., II.; Helser, A.; Chi, V.; Brooks, F. P., Jr.; Washburn, S.; Superfine, R. *Nature* **1999**, *397*, 236−238.
(18) Fujikawa, Y.; Sadowski, J. T.; Kelly, K. F.; Nakayama, K. S.; Mickelson, E. T.; Hauge, R. H.; Margrave, J. L.; Sakurai, T. *Jpn. J. Appl. Phys.* **2002**, *41*, 245−249.
(19) Yamachika, R.; Grobis, M.; Wachowiak, A.; Crommie, M. F. *Science* **2004**, *304*, 281−284.
(20) Synthesis of nanocar **1** and trimer **2** and **3**. Commercially available **4** was iodinated and coupled with trimethylsilyl aecetylene (TMSA) using Pd/Cu catalysis, and then the amino group was converted to an iodide for the subsequent coupling reaction with axle unit **6**. The bromide to iodide conversion (**7** to **8**) was required for a successful coupling reaction with the middle chassis, **9**. Further coupling with axle unit **11** yielded **12**. After the removal of silyl-protecting groups with tetrabutylammonium fluoride (TBAF), four fullerene-C_{60}s were coupled via an in situ ethynylation method[21] to complete the synthesis of nanocar **1**. Note: Pd/Cu = $PdCl_2(PPh_3)_2$ and CuI. FTIR (CH_2Cl_2, cast) 2922, 2850, 2203, 1502, 1463, 1214 cm^{-1}; ^1H NMR (500 MHz, $CDCl_3$): δ 7.77 (d, $J = 1.4$ Hz, 2H), 7.58 (d, $J = 8.0$ Hz, 2H), 7.51 (dd, $J = 8.0$ Hz, 1.4 Hz, 2H), 7.30 (s, 2H), 7.25 (s, 2H), 7.18 (s, 2H), 7.15 (s, 2H), 7.14 (s, 2H), 7.10 (s, 2H), 7.07 (s, 2H), 7.03 (s, 2H), 4.19−4.14 (m, 8H), 4.09 (m, 4H), 4.00 (m, 4H), 3.90−3.88 (m, 8H), 1.95−1.13 (m, 192H), 0.88−0.80 (m, 36H); ^{13}C NMR (125 MHz, $CDCl_3$): δ 154.7, 154.6, 153.9, 153.75, 153.67, 153.65, (6 signals from sp^2-*C*O in the aromatic ring), 151.65, 151.59, 151.497 (×2), 147.7 (×2), 147.44, 147.43, 146.74, 146.69, 146.50, 146.477 (×2), 146.46, 146.32 (×2), 146.31 (×2), 145.92, 145.89, 145.82, 145.77, 145.72, 145.69, 145.55, 145.529 (×2), 145.51, 145.45, 145.43, 144.78, 144.76, 144.60, 144.58, 143.28, 143.26, 142.69, 142.67, 142.66, 142.64, 142.21, 142.17, 142.13, 142.11, 142.07, 142.05, 141.98, 141.95, 141.77, 141.73, 141.69, 141.67, 140.47, 140.44, 140.40, 140.37, 136.18, 136.15, 135.3, 135.2, (30 × 2 signals from sp^2-C in the C_{60} core), 134.4, 131.6, 130.9, 126.5, 125.8, 123.3, 117.6, 117.4 (×2), 117.2, 117.0, 116.9, 114.9, 114.7, 114.4, 114.2, 113.4, 113.2, 97.8, 96.1, 94.3, 94.1, 93.1, 92.2, 91.8, 91.0, 88.3, 80.2 (×2), 70.14, 70.10, 69.8, 69.6, 69.5, 69.3, 62.02 and 61.98 (2 signals from *C*H in the C_{60} core), 55.60 and 55.59 (2 signals from quaternary sp^3-C in the C_{60} core), 32.04, 31.97, 31.95, 29.8, 29.74, 29.70, 29.66, 29.48, 29.45, 29.40, 22.77, 22.75, 22.73, 14.23, 14.21, 14.19; MALDI-TOF MS (sulfur as the matrix) calcd for $C_{430}H_{274}O_{12}$, 5632; found, *m/z*: 5631 [M^+]. Trimers **2** and **3** were prepared as described following a related protocol.[21]
(21) (a) Shirai, Y.; Zhao, Y.; Cheng, L.; Tour, J. M. *Org. Lett.* **2004**, *6*, 2129−2132. (b) Zhao, Y.; Shirai, Y.; Slepkov, A. D.; Cheng, L.; Alemany, L. B.; Sasaki, T.; Hegmann, F. A.; Tour, J. M. *Chem.−Eur. J.* **2005**, *11*, 3643−3658.
(22) Kanno, T.; Tanaka, H.; Nakamura, T.; Tabata, H.; Kawai, T. *Jpn. J. Appl. Phys.* **1999**, *38*, L606-L607.
(23) Terada, Y.; Choi, B. K.; Heike, S.; Fujimori, M.; Hashizume, T. *Nano Lett.* **2003**, *3*, 527−531.
(24) Chase, S. J.; Bacsa, W. S.; Mitch, M. G.; Pilione, L. J.; Lannin, J. S. *Phys. Rev. B* **1992**, *46*, 7873−7877.
(25) Altman, E. I.; Colton, R. J. *Surf. Sci.* **1993**, *295*, 13−33.
(26) Tzeng, C.-T.; Lo, W.-S.; Yuh, J.-Y.; Chu, R.-Y.; Tsuei, K.-D. *Phys. Rev. B* **2000**, *61*, 2263−2272.
(27) Pascual, J. I.; Jackiw, J. J.; Kelly, K. F.; Conrad, H.; Rust, H.-P.; Weiss, P. S. *Phys. Rev. B* **2000**, *62*, 12632−12635.
(28) Hofer, W. A.; Foster, A. S.; Shluger, A. L. *Rev. Mod. Phys.* **2003**, *75*, 1287−1331.
(29) Jung, T. A.; Schlittler, R. R.; Gimzewski, J. K.; Tang, H.; Joachim, C. *Science* **1996**, *271*, 181−184.
(30) Gimzewski, J. K.; Joachim, C. *Science* **1999**, *283*, 1683−1688.

NL051915K